Publications of the Astronomical Society of Australia (2026), **43**, e055, 8 pages
doi:10.1017/pasa.2026.10189

CAMBRIDGE UNIVERSITY PRESS

Research Article

Eccentric millisecond pulsar + subdwarf B star from rotationally delayed accretion-induced-collapse scenario

Xiangcun Meng

International Centre of Supernovae (ICESUN), Yunnan Key Laboratory of Supernova Research, Yunnan Observatories, Chinese Academy of Sciences (CAS), Kunming 650216, China

Abstract

Eccentric millisecond pulsar + helium white dwarf (MSP + He WD) systems have attracted increasing attention, with the rotationally delayed accretion-induced collapse (RD-AIC) scenario proposed as a possible formation channel. Given the similarity between the formation channels of He WDs and subdwarf B (sdB) stars, eccentric MSP + sdB binaries could also exist in the Galaxy, though none have been detected so far. Theoretical predictions of their properties would greatly aid in their discovery. Here, within the RD-AIC framework, I present predictions for their orbital parameters, including MSP mass, secondary mass, eccentricity, and orbital period. Based on two detailed binary population synthesis calculations, I estimate their Galactic birth rate to be $(0.67–1.5) \times 10^{-4}\mathrm{yr}^{-1}$. Then, a very conservative upper limit for their total number in the Galaxy is 15 000, implying that the most optimistic fraction of eccentric MSP + sdB systems among all MSP + sdB populations could reach up to 55%. These systems are relatively young, with ages on the order of a few hundred Myr, and should therefore be found in relatively young environments. Furthermore, most MSPs in such eccentric binaries have masses below 1.5 $M_{\odot}$. I also briefly discuss their potential future applications in various astrophysical contexts.

Keywords: (stars:) Subdwarfs; white dwarfs; binaries: general

(Received 11 December 2025; revised 4 March 2026; accepted 6 April 2026)

1. Introduction

Millisecond pulsars (MSPs) are characterised by weak surface magnetic fields of $B \sim 10^8$ G, spin periods shorter than 30 ms, period derivatives less than $10^{-19}\mathrm{s\,s}^{-1}$ and nearly circular orbits. They play a vital role in constraining the equation of state (EoS) of neutron stars (NSs, Özel & Freire 2016). The prevailing view is that MSPs form in low-mass X-ray binaries (LMXBs) through a recycling process: a pulsar that has crossed the death line is spun up to millisecond periods via accretion from a Roche lobe–filling companion. (Alpar et al. 1982; Radhakrishnan & Srinivasan 1982; Bhattacharyya & van den Heuvel 1991). Tidal torques during this phase circularise the binary orbit (Phinney & Kulkarni 1994). This scenario is supported by observed links between LMXBs and MSPs (Wijnands & van der Klis 1998; Archibald et al. 2009), as well as the fact that nearly all fully recycled MSPs with helium white dwarf (WD) companions in the Galaxy exhibit very low orbital eccentricities (Manchester et al. 2005).

However, the detection of several eccentric MSPs suggests that the recycling process may be more complex than previously envisioned. These eccentric MSPs are found with either main-sequence (MS) stars or low-mass helium WDs as companions (Champion 2008; Barr et al. 2017; Octau et al. 2018; Stovall et al. 2019; Zhu et al. 2019; Serylak et al. 2022). While several formation mechanisms have been proposed, the origin of such systems remains uncertain. Most models invoke either asymmetric mass loss or environmental interactions: (I) Dynamical perturbations in a hierarchical triple system may eject one component, leaving an eccentric binary (Freire et al. 2011). (II) A circumbinary (CB) disk formed from mass loss in the progenitor system may interact with the inner binary, exciting orbital eccentricity (Antoniadis 2014). (III) Asymmetric mass ejection during proto-WD formation could impart a kick, resulting in an eccentric MSP binary (Han & Li 2021; Tang, Gao, & Li 2023). (IV) The accretion-induced collapse (AIC) of a rapidly rotating super-Chandrasekhar WD could directly produce an MSP, with mass loss inducing eccentricity (Freire & Tauris 2014; Wang & Gong 2023). (V) Similarly, a phase transition from a rapidly rotating NS to a strange star, accompanied by sudden mass loss, may also yield an eccentric MSP binary (Jiang et al. 2015). (VI) Resonant interaction with convective flows in a tidally locked red giant, when the eddy turnover time matches the spin period, could drive large eccentricities (Ginzburg & Chiang 2022).

Hot subdwarfs, identified as extreme horizontal branch (EHB) stars in the Hertzsprung–Russell (HR) diagram, are helium-core-burning objects with very thin hydrogen envelopes (Heber 2009; Heber 2016). Like helium WDs, they typically form from red giants that have lost their hydrogen envelopes. Hot subdwarfs are important in several astrophysical contexts, for instance, as contributors to the ultraviolet upturn in elliptical galaxies and as potential surviving companions of Type Ia supernovae (Han, Podsiadlowski, & Lynas-Gray 2007; Geier et al. 2015; Meng & Luo 2021). After central helium exhaustion, hot subdwarfs evolve into carbon-oxygen (CO) WDs, including very low-mass WDs with CO cores (Prada Moroni & Straniero 2009; Justham, Podsiadlowski, & Han 2011). Spectroscopically, they are classified

Email: xiangcunmeng@ynao.ac.cn

Cite this article: Meng X. (2026) Eccentric millisecond pulsar + subdwarf B star from rotationally delayed accretion-induced-collapse scenario. *Publications of the Astronomical Society of Australia* **43**, e055, 1–8. https://doi.org/10.1017/pasa.2026.10189

© The Author(s), 2026. Published by Cambridge University Press on behalf of Astronomical Society of Australia. This is an Open Access article, distributed under the terms of the Creative Commons Attribution licence (https://creativecommons.org/licenses/by/4.0/), which permits unrestricted re-use, distribution and reproduction, provided the original article is properly cited.

into several subtypes, e.g. the dominant subgroup, subdwarf B (sdB) stars, exhibits strong hydrogen Balmer lines and weak or absent He I lines (Moehler et al. 1990; Geier et al. 2017; He et al. 2025).

Although neutron stars can, in principle, have diverse companions, no NS binaries with helium-star or hot subdwarf companions had been identified until 2025. Recently, however, NS + hot subdwarf systems have attracted growing theoretical and observational interest. They are potential gravitational wave sources detectable by the Laser Interferometer Space Antenna (LISA) and may represent progenitors of certain peculiar MSP binaries, such as those with CO WD companions or black widows with extremely low-mass companion (Tauris, Langer, & Kramer 2012; Wu et al. 2018; Ginzburg & Chiang 2020; Guo, Wang, & Li 2024). For over a decade, several surveys have sought such binaries to understand their apparent rarity and evolutionary pathways (e.g. Geier et al. 2011; Wu et al. 2020).

The recent report of a compact binary comprising an MSP and a stripped helium star, the first of its kind, has reinvigorated this field (Yang et al. 2025). This system, consistent with standard recycling predictions, exhibits a circular orbit (Guo et al. 2025). Yet, given that eccentric MSP + He WD systems, though rare, challenge the standard recycling picture, new questions have emerged: Do eccentric MSP + hot subdwarf systems also exist, in contradiction to standard recycling predictions? If so, how many such systems reside in the Galaxy, what are their characteristic properties, and in what kind of environments within the Milky Way can they be discovered? In this paper, I address these questions by predicting the properties of potential eccentric MSP + hot subdwarf binaries. Such predictions will facilitate future searches for these systems, whose discovery could provide strong constraints on the standard recycling theory.

In studies of the properties of the surviving companions of Type Ia supernovae (SNe Ia) in supernova remnants (SNRs), the so-called spin-up/spin-down model suggests that the companion of a rapidly rotating CO WD prior to explosion could be an sdB star (Justham 2011; Di Stefano & Kilic 2012; Meng & Li 2019). If the WD is composed of oxygen–neon–magnesium (ONeMg), AIC may occur instead of a SN Ia. While direct evidence for AIC events remains elusive, indirect observational clues support this channel, e.g. the young pulsars in globulars clusters (Tauris et al. 2013; Wang & Liu 2020; Kremer et al. 2024). As discussed in Section 4.1, the rotationally delayed AIC (RD-AIC) scenario proposed by Freire & Tauris (2014) offers a promising explanation for known eccentric MSP + He WD systems. If the RD-AIC scenario is valid, the outcome of an AIC event in a rapidly rotating ONeMg WD + sdB binary would be an eccentric MSP + sdB system, or at least an eccentric NS + sdB binary. This work aims to characterise such yet-undetected eccentric MSP + sdB systems and provide observable predictions to guide future searches (Oostrum et al. 2020).

In Section 2, I simply describe my methods, and I present the results in Section 3. In Section 4, I show discussions and my main conclusions.

2. Methods

As far as the potential eccentric MSP + sdB systems from the RD-AIC scenario, their lifetimes may be much shorter than normal MSPs from recycled scenario because massive WDs tend to have higher magnetic fields (10^6–10^9 G, Wickramasinghe & Ferrario 2005), which leads to the post-AIC MSPs with a strong magnetic field of 10^{11}–10^{14} G, as high as magnetar. Only those from the WDs with very weak magnetic fields may show the properties of normal MSPs (see also Ivanova et al. 2008). Here, I simply assume that a post-AIC NS behaves as a MSP no matter how strong its magnetic field is, and then how long its lifetime. I will discuss this further in Section 4.

Following Meng & Li (2019), the initial binary systems are ONeMg WD + MS systems, and mass transfer begins when the companions are on the MS or in the Hertzsprung gap (HG) (see also details in Meng & Podsiadlowski 2017). The basic methods and assumptions for the binary evolution are the same to Meng & Li (2019) before AIC, and then I do not give the repetitious details here. As far as the maximum WD is concerned, a rigid rotation is assumed for the pre-AIC WD and then the maximum WD mass is 1.48 $M_\odot$ in Freire & Tauris (2014) (see Meng & Li 2019 and Tauris et al. 2013). Actually, if a differential rotation is considered, the maximum mass may be up to 4.0 $M_\odot$ (Yoon & Langer 2004; Yoon & Langer 2005). In this paper, I assume that the pre-AIC WD may be differentially rotating if its mass exceeds 1.48 $M_\odot$. The WD mass in this paper is then as massive as 2.6 $M_\odot$. The rapidly rotating super-Chandrasekhar WDs will experience a spin-down phase before an AIC process. However, at present, many uncertainties are still not resolved in the spin-up/spin-down model, e.g. the exact spin-down timescale and the exact time of the onset of the spin-down phase (Meng & Podsiadlowski 2013). Following Meng & Li (2019) and Meng & Luo (2021), I define a pseudo-spin-down timescale, $\tau_{\rm sp} = 10^7$ yr, in which $\tau_{\rm sp}$ represents a time interval from the moment of $M_{\rm WD} = 1.378\ M_\odot$ to the time of AIC (see also Meng & Podsiadlowski 2013).[a] For the AIC process, I take similar assumptions to those in Freire & Tauris (2014). (i) The binding energy of a NS is calculated based on Lattimer & Yahil (1989) and the baryonic material of 0.02 $M_\odot$ is ejected during AIC (Wang & Liu 2020). (ii) I assume a circular orbit for the pre-AIC binary. If the AIC is symmetric, I use

$$e = \frac{\Delta M}{M_{\rm NS} + M_2}, \tag{1}$$

to calculate the eccentricity of the post-AIC system, where M_2, $M_{\rm NS}$ and ΔM are the pre-AIC secondary mass, the post-AIC MSP mass and the mass loss during AIC, respectively (Bhattacharyya & van den Heuvel 1991). This means that the effect of the ejected baryonic material on the companion is neglected because of its small amount. I calculate the post-AIC semimajor axis, a, by

$$\frac{a}{a_0} = \frac{M_0 - \Delta M}{M_0 - 2\Delta M}, \tag{2}$$

and then calculate the orbital period of the post-AIC systems according to a, where a_0 and M_0 are the orbital separation and the total mass of the pre-AIC system (Hills 1983). (iii) Following the formulae in Hills (1983), I also discuss the dynamical effect of asymmetrical AIC on the post-AIC systems by a Monte Carlo way (see detailed discussions in Freire & Tauris 2014).

Based on the calculations in Meng & Li (2019), I may get the parameter space in the initial orbital period – secondary mass plane in which an ONeMg WD + MS system may become an eccentric MSP + sdB system after AIC. To obtain the birth rate of the eccentric MSP + sdB systems, I made two binary population synthesis (BPS) calculations using the rapid binary evolution code developed by Hurley, Pols, & Tout (2000), Hurley, Tout, & Pols (2002). I assume that if the initial orbital period, $P^i_{\rm orb}$, and the

[a]Here, the real spin-down timescale is generally longer than 9×10^6 yr, since the mass transfer timescale is generally shorter than 10^6 yr.

https://doi.org/10.1017/pasa.2026.10189 Published online by Cambridge University Press

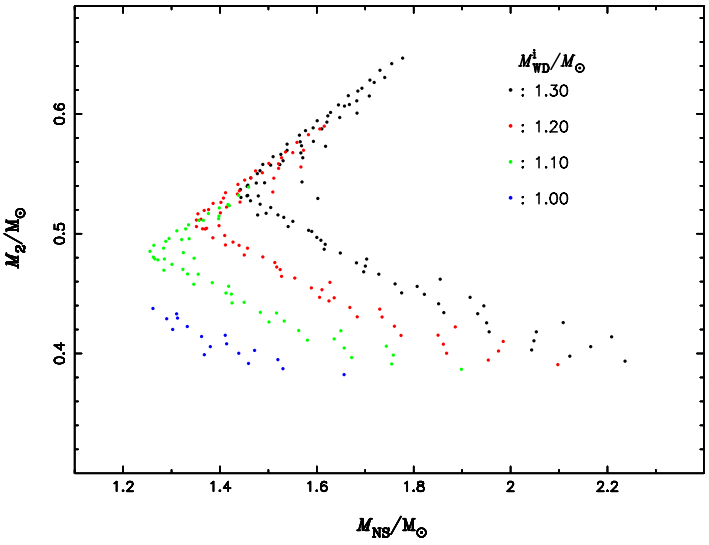


Figure 1. The masses of two components of the eccentric MSP + sdB systems for different initial WD masses.

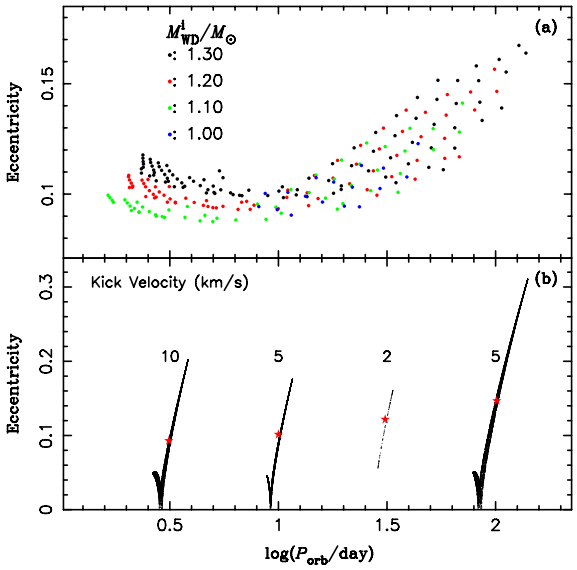


Figure 2. Panel (a): Eccentricities vs orbital periods of the systems from the RD-AIC scenario for different initial WD masses, where a symmetric collapse is assumed. Panel (b): Distributions of the eccentricities and orbital periods of the post-AIC systems from the pre-AIC systems of [$M_{WD}/M_\odot$, $M_2/M_\odot$ log (P/day)] = (1.5063, 0.4958, 0.4128), (1.6829, 0.53‘5, 0.9115), (1.9070, 0.4046, 1.3820) and (2.3358, 0.4101, 1.8727), respectively. The stars indicate the systems without kick, while the others show the distributions of the eccentricities and orbital periods of the systems with different small kick velocities in unit of km/s as shown by the numbers, where the direction of the kick velocity is generated by a Monte-Carlo way.

initial secondary mass, M_2^i, of an ONeMg WD + MS system are located in the appropriate region in the ($\log P^i - M_2^i$) plane for the eccentric MSP + sdB systems at the onset of Roche lobe overflow (RLOF), an eccentric MSP + sdB system can be produced. I followed the evolution of 10^8 sample binaries, where the primordial binary samples are generated in a Monte Carlo way. The assumptions and the input parameters for the Monte Carlo simulations are the same to that in Meng & Podsiadlowski (2017), and I do not show the repetitious details here. As I will show in the next section, the common-envelope (CE) ejection efficiency, α_{CE}, is a very important parameter to affect the birth rate of the eccentric MSP + sdB systems. Following Meng & Podsiadlowski (2017), I take $\alpha_{CE} = 1.0$ or $\alpha_{CE} = 3.0$ (see Meng & Podsiadlowski 2017 for details)

3. Results

3.1. Properties of the eccentric MSP + sdB systems

Measuring the mass of a massive NS is a very important way to constrain the EoS of NSs, and a significant progress has been made in this field (Demorest et al. 2010; Cromartie et al. 2020). In Figure 1, I show the masses of MSPs and sdB stars in eccentric binaries from the RD-AIC scenario for different initial WD masses. As shown in the figure, the MSPs have a mass between 1.25 and 2.2 $M_\odot$. The maximum MSP mass here is much larger than that in Freire & Tauris (2014) just because I assume that the pre-AIC WD may be differentially rotating. The sdB stars have a mass from 0.38 to 0.65 $M_\odot$ as standard binary model predicted (Han et al. 2003). In the ($M_{NS} - M_2$) plane, the systems are clearly divided into two branches, which are derived from the different evolutionary stages of the companions and differences in mass-transfer rates at the onset of RLOF for initial WD + MS systems (see detailed explanation in Meng & Podsiadlowski 2017)

In Figure 2, I show the distribution of the eccentricities and the orbital periods of the post-AIC systems. For a symmetric-collapse assumption (panel a), the RD-AIC scenario leads to a very narrow range of post-AIC eccentricities: 0.09–0.17, which is slightly larger than that of the eccentric MSP + He WD systems from the RD-AIC scenario because of a more massive pre-AIC WD (Freire & Tauris 2014). However, the post-AIC orbital periods here range from ∼1.6 to ∼150 d which is much larger than that for eccentric MSP + He WD systems. The orbital period of a post-AIC system mainly depends on its pre-AIC binary evolution and then on the initial binary parameters of a WD + MS system (see also Meng & Luo 2021).

The eccentricity and orbital period of a post-AIC system is quite sensitive to a kick to the MSP during the AIC. I use the formulae in Hills (1983) to check the potential dynamical effect to four different systems by assuming different small kick velocities, where the direction of the kick velocity is generated by a Monte-Carlo way. The results are shown in the panel (b) of Figure 2. Similar to that in Freire & Tauris (2014), the eccentricity and the orbital period of a given system distribute in a $\surd$-shape region in the ($e - \log P_{orb}$) plane for a relatively larger kick velocity, while in a narrow strip for a relatively smaller kick velocity. The panel (b) shows that for a system with an asymmetrical AIC, the post-AIC eccentricity may be as large as 0.3, even though the kick velocity is as small as 5 km s^{-1}. In addition, as expected in the formulae of Hills (1983), for a given value of the kick velocity, the longer the pre-AIC orbital period, the larger the maximum of and then the range of the post-AIC eccentricity.

According to the model grid calculations in Meng & Li (2019), in Figure 3 I show the parameter spaces in ($M_2^i - \log P^i$) plane, in which a ONeMg WD + MS system is assumed to lead to an eccentric MSP + sdB system via the RD-AIC scenario. Comparing with the parameter spaces for SNe Ia, the parameter spaces leading to the eccentric MSP + sdB systems locate at the right-upper region, i.e. their initial orbital periods are longer than 3 d and initial companion is more massive than 2.5 $M_\odot$, which indicates that the

https://doi.org/10.1017/pasa.2026.10189 Published online by Cambridge University Press

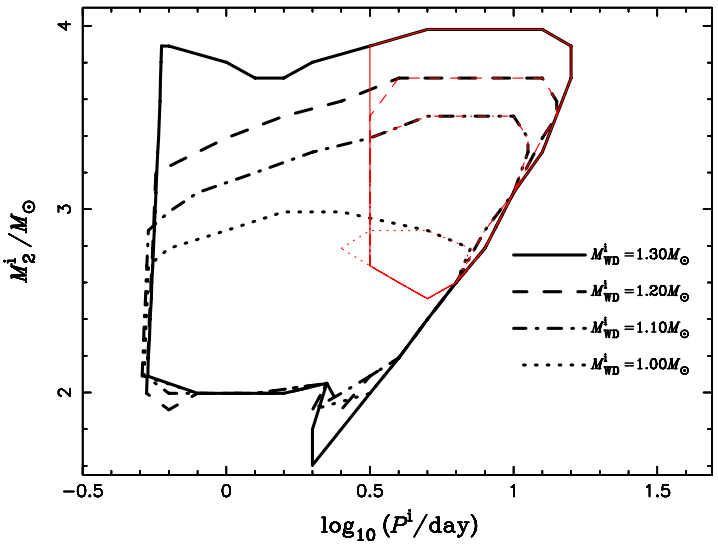


Figure 3. The parameter spaces in (M_2^i – log P^i) plane for different initial WD masses, in which a ONeMg WD + MS system may lead to an eccentric NS + sdB system via RD-AIC scenario (red lines). The black lines are those for SNe Ia from Meng & Podsiadlowski (2017, 2018).

eccentric MSP + sdB systems from the RD-AIC scenario belong to relatively young population.

3.2. Birth rate of eccentric MSP + sdB systems

Based on the parameter spaces, I carried out two BPS calculation to obtain the birth rate of the eccentric MSP + sdB systems. In the Figure 4, I show the evolution of the birth rates, ν, of the eccentric MSP + sdB systems from the RD-AIC scenario for a constant Galactic star formation rate of SFR = 5 $M_\odot$ yr^{-1} (top panel) and a single starburst of 10^{11} $M_\odot$ (bottom panel). The Galactic birth rate of these systems is then (0.67–1.5) × 10^{-4}yr^{-1}, which is significantly smaller than the total birth rate of AIC events (Wang 2018). Then, the number of the eccentric MSP + sdB systems may be calculated by $\nu \times \tau_{\rm MSP}$, where $\tau_{\rm MSP}$ is the lifetime of the eccentric MSP + sdB systems. Assuming an optimistic lifetime of 10^8 yr for the MSPs with strong magnetic fields and a typical life of 10^8 yr for a sdB star (Ivanova et al. 2008), the number of the eccentric MSP + sdB systems in the Galaxy is then 6 700–15 000, which is similar to that of NS + sdB systems from core collapse supernovae (Wu et al. 2020). The delay time for the eccentric MSP + sdB systems is between 160 and 630 Myr and the peak of the birth rate for a single starburst locates at ∼300 Myr (bottom panel). So, these systems belong to relatively young population as their progenitor systems indicate. Assuming the lifetime of 10^8 yr for sdB stars and MSPs with strong magnetic fields, there are (6–15) such systems in a cluster of 10^6 $M_\odot$ with an age of ∼300 Myr. This number is much smaller than that of total AIC events in a cluster (Ivanova et al. 2008). Considering that the dynamical interaction is very efficient in a cluster and then the eccentric MSP + sdB systems with a long orbital period are likely to be disrupted and to possibly form isolated MSPs, such a number estimation could even be too optimistic. I address this issue in Section 4 again.

3.3. Distribution of WDs

The main different assumptions between this paper and Freire & Tauris (2014) is that the WDs before AIC may be differential rotating, rather than just rigid rotating, and then the WD before

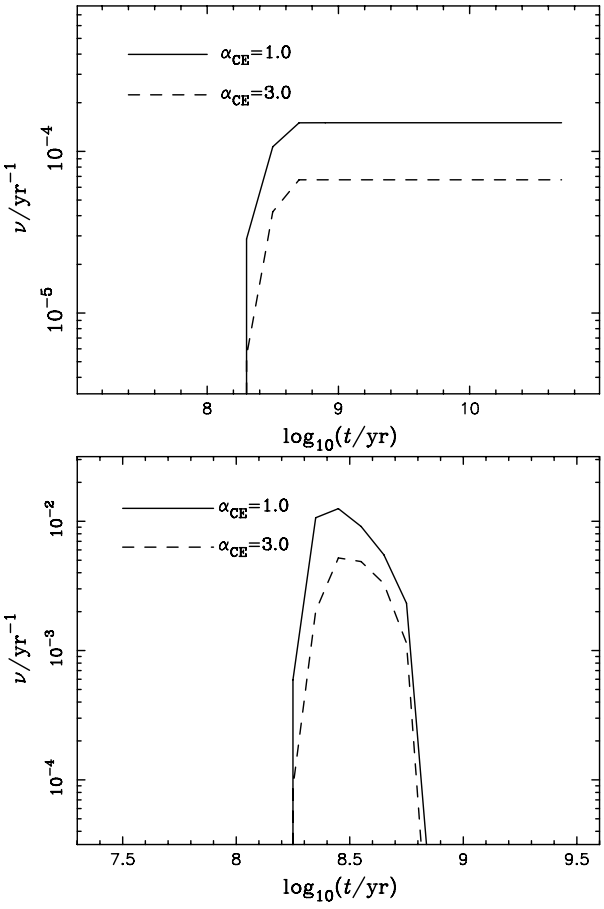


Figure 4. The evolution of the birth rates, ν, of the eccentric MSP + sdB systems from the RD-AIC scenario for two values of $\alpha_{\rm CE}$ and a constant star formation rate of SFR = 5 $M_\odot$ yr^{-1} (top panel), or a single starburst of 10^{11} $M_\odot$ (bottom panel).

AIC may be more massive than 1.48 $M_\odot$. However, there might be various efficient angular momentum transfer mechanisms, which means that different rotation patterns would be possible. Generally speaking, the WDs are rigid rotating before AIC if their masses are smaller than 1.48 $M_\odot$. Therefore, the mass distribution of white dwarfs prior to AIC may reveal the importance of rigidly rotating white dwarfs in the formation of eccentric MSP + sdB systems. In Figure 5, I show the distribution of initial WD mass and the WD mass before AIC for different $\alpha_{\rm CE}$. It is clearly shown in the top panel of Figure 5 that a smaller $\alpha_{\rm CE}$ leads to the peak of the initial WD mass distribution to move to a higher value. This is derived from a fact that all the systems experience a CE phase before they become the ONeMg WD + MS systems. A system with a less massive WD is more likely to merge for a smaller $\alpha_{\rm CE}$ value after a common envelope phase, i.e. as a result, a system with a more massive WD is more likely to survive from the common envelope evolution and then becomes a potential progenitor system of an eccentric MSP + sdB system.

For the distribution of the WD mass before AIC, three properties are worthy to be noticed in the bottom panel of Figure 5. First, only about 5%–14% WDs have a mass less than 1.48 $M_\odot$, which indicates that the rigid rotation is not a dominant case for the AIC channel. This is mainly from the fact that an ONeMg WD generally has a large initial mass and then is easy to exceed the limit of the rigid rotation after a mass transfer occurs between the WD and its massive companion (more massive than 2.5 $M_\odot$ and see also Figure 3). Second, the peak of the distribution moves to a

https://doi.org/10.1017/pasa.2026.10189 Published online by Cambridge University Press

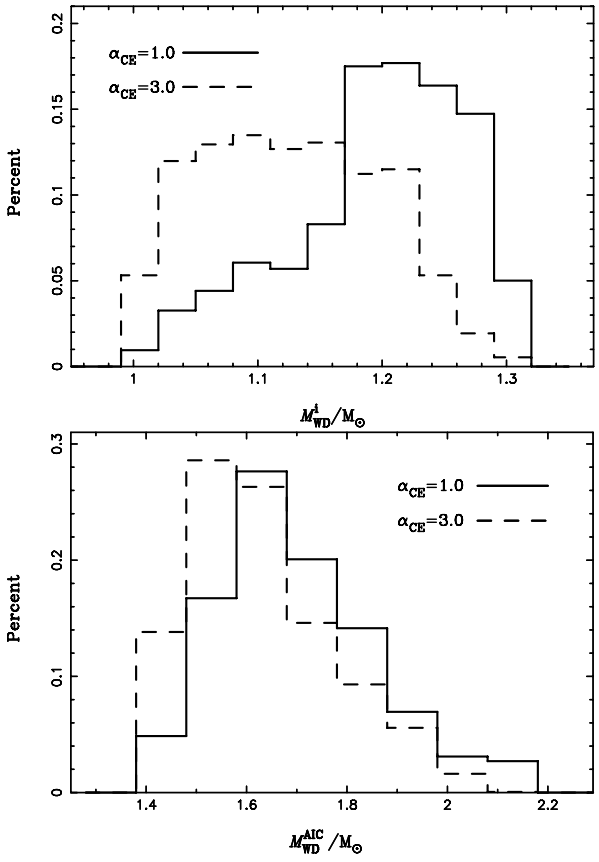


Figure 5. The distribution of the initial WD mass (top panel) and the WD mass before AIC (bottom panel) for two values of α_{CE}.

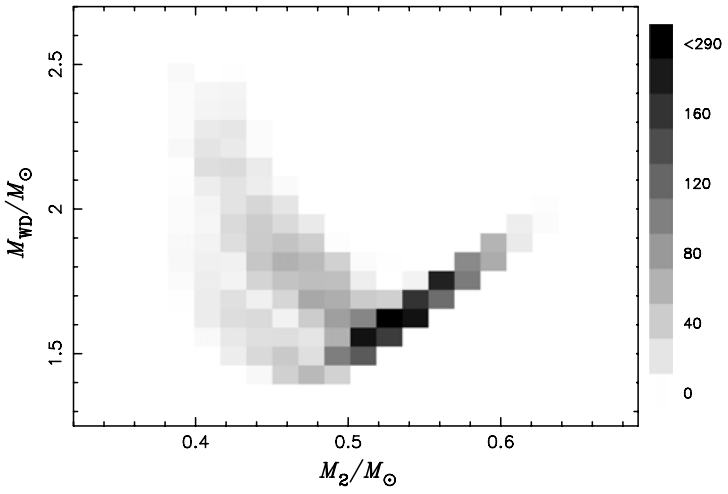


Figure 6. The distributions of WD and sdB masses at the moment of AIC in the $M_{WD} - M_2$ plane, where $\alpha_{CE} = 1.0$. The basic properties for the case of $\alpha_{CE} = 3.0$ is similar.

lower value for a higher α_{CE}, which is directly correlated with the distribution of the initial WD mass (see the top panel of Figure 5). Third, about 50%–70% WD have a mass less massive than about 1.68 $M_{\odot}$ and only about 2%–7% WDs have a mass more massive than 2 $M_{\odot}$, although in principle, a 2.6 $M_{\odot}$ WD is possible before AIC. This means that most of the MSPs in the eccentric MSP + sdB systems have a mass less massive than ∼1.5 $M_{\odot}$, which provides another information to be verified by a large sample of the eccentric MSP + sdB systems in the future.

Figure 6 presents the distributions of WD and its companion masses at the moment of AIC in the $M_{WD} - M_2$ plane. Here, I only present the case of $\alpha_{CE} = 1.0$ and the case of $\alpha_{CE} = 3.0$ is similar to that. According to Figure 6, readers may also obtain the distributions of the MSP and sdB masses in eccentric MSP + sdB systems in a $M_{NS} - M_2$ plane, as shown in Figure 1. Similar to Figure 1, the systems are also clearly divided into two branches in the M_{WD}-M_2 plane, i.e. no system locates at the region around $M_{WD} \sim 2.1$ $M_{\odot}$ and $M_2 \sim 0.52$ $M_{\odot}$. For the WDs of less than 1.5 $M_{\odot}$, the masses of sdB stars focus on ∼ 0.5 $M_{\odot}$, while for the WDs of higher than 2.0 $M_{\odot}$, the sdB stars have a mass less than 0.48 $M_{\odot}$. The two-branch distribution here provides a way to examine the predictions in this paper by a large sample in the future.

4. Discussions and conclusions

In this study, inspired by the suggestion of Freire & Tauris (2014) that the RD-AIC scenario may account for the formation of eccentric MSP + He WD systems, I estimate that there could be 6 700–15 000 eccentric MSP + sdB systems in the Galaxy. Their orbital parameters are also predicted; for instance, under the assumption of symmetric collapse, their eccentricities lie between 0.09 and 0.17 (see Figures 1 and 2), with most MSPs having masses below 1.5 $M_{\odot}$. The formation of such systems requires mass transfer to initiate during the HG phase in an initial ONeMg WD + MS binary. The delay time for their emergence is on the order of several hundred Myr, peaking at ∼300 Myr. Therefore, these systems are expected to be found in relatively young environments such as the Galactic thin disk. In particular, if the associated AIC involves only a low kick velocity, the resulting systems are likely to possess low peculiar velocities and follow disk-like orbits in the Galaxy. A future detection of eccentric MSP + sdB binaries would thus offer additional indirect evidence in support of the AIC process.

4.1. Eccentric MSP + He WD systems

To account for the observed properties of the eccentric MSP + He WD systems, Freire & Tauris (2014) adopt a WD delay time longer than 10^9 yr, while a pseudo-spin-down timescale of 10^7 yr is assumed in this work. The extended delay time in Freire & Tauris (2014) is motivated by two considerations. First, prior to AIC, the red giant companion is assumed to evolve into a white dwarf, terminating mass transfer. Consequently, after AIC, the resulting eccentric MSP + He WD system may retain its orbital eccentricity. Second, a longer delay allows the super-Chandrasekhar WD sufficient time to cool before undergoing RD-AIC. Furthermore, Freire & Tauris (2014) assume rigidly rotating super-Chandrasekhar ONeMg WDs, which restricts their masses to below 1.48 $M_{\odot}$ (Yoon & Langer 2004). In contrast, our model incorporates differentially rotating WDs, permitting masses exceeding 2 $M_{\odot}$, as illustrated in Figures 5 and 6. If our assumptions prove viable for eccentric MSP + sdB systems, they may, in principle, also offer a plausible explanation for the observed eccentric MSP + He WD systems.

The assumed spin-down timescale of 10^7 yr is consistent with, and at least does not conflict with, the two constraints mentioned above. First, a delay time of ∼10^7 yr is certainly sufficient to allow a WD of ∼0.3 $M_{\odot}$ to enter the cooling branch of WD before AIC occurs (Chen, Meng, & Han 2017; Chen et al. 2017). Second,

https://doi.org/10.1017/pasa.2026.10189 Published online by Cambridge University Press

although the timescale to undergo RD-AIC remains highly uncertain, i.e. in a range of 10^5–10^9 yr, depending on the redistribution of angular momentum within super-Chandrasekhar ONeMg WDs (Yoon & Langer 2004, 2005), it is still plausible for an AIC to occur in a super-Chandrasekhar ONeMg WD in $\sim 10^7$ yr, particularly in systems hosting WDs as massive as 2.4 $M_\odot$ (Hachisu et al. 2012; also Meng & Podsiadlowski 2013).

The mass of a NS in an eccentric binary system can be determined through measurements of relativistic Shapiro delay or the rate of advance of periastron (Demorest et al. 2010; Özel & Freire 2016; Cromartie et al. 2020). While some properties of MSP systems are well explained by the RD-AIC scenario (Freire & Tauris 2014; Wang & Gong 2023), others remain challenging, for instance, some observed pulsar masses substantially exceed the predictions under the rigid-rotation RD-AIC hypothesis proposed by Freire & Tauris (2014) (Barr et al. 2017; Serylak et al. 2022). If eccentric MSP systems originate from a differential-rotation RD-AIC channel, the orbital eccentricity could be used to infer the pre-AIC WD mass of the NS via Equation (1). Consequently, the measurement of the NS mass and the eccentricity may shed light on the formation origin of eccentric MSPs. As an illustration, Figure 7 presents the relation between pre-AIC WD mass and post-AIC NS mass under the assumption of symmetric collapse, alongside observational data for eccentric MSP + He WD systems (also assuming symmetric collapse). These systems align closely with the theoretical relation predicted by the RD-AIC scenario, suggesting that provided differentially rotating ONeMg WDs exist, such systems could indeed originate from RD-AIC. Similarly, future discoveries of eccentric MSP + sdB systems could further help to clarify the origin of eccentric MSP + He WD binaries. Another noteworthy feature in Figure 7 is that three of the five observed eccentric MSP + He WD systems contain MSPs with masses below 1.5 $M_\odot$, consistent with the prediction shown in Figure 5. This highlights the need for future detailed BPS studies that incorporate differential rotation, rather than relying solely on rigid-rotation assumptions (e.g. Wang & Gong 2023). Additionally, detailed binary evolution calculations confirm that super-Chandrasekhar WDs exceeding 2 $M_\odot$ indeed form from WD + red giant systems when differential rotation is taken into account (Chen et al. 2017). Finally, the slight deviation of PSR J1950+2414 from the theoretical relation in Figure 7 may indicate the presence of a small kick imparted to the MSP during the AIC process.

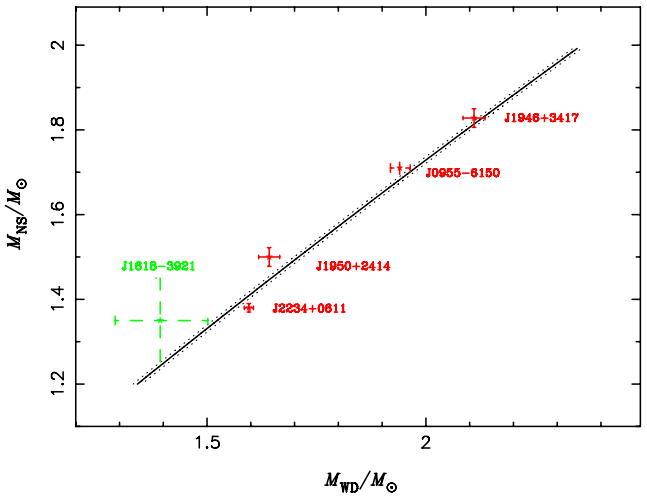


Figure 7. Pre-AIC WD mass vs. post-AIC NS mass with an assumption of differential rotation, symmetric collapse and ejection of baryonic material of 0.02 $M_\odot$ (solid line), or 0.01 and 0.03 $M_\odot$ (dotted line), respectively. The stars present observed results, where the symmetric collapse is assumed. Red stars show the systems with precise measurement of NS mass and eccentricity, while the green one shows the results where the NSs are assumed to have a mass of 1.25–1.45 $M_\odot$ with a median of 1.35 $M_\odot$ and the companions are assumed to be He WDs. The observational dada are from Barr et al. (2017), Octau et al. (2018), Stovall et al. (2019), Zhu et al. (2019) and Serylak et al. (2022).

4.2. *Uncertainties and potential applications for eccentric MSP + sdB systems*

Compared to the circular MSP + He WD binaries, systems with eccentric orbits are exceptionally rare, accounting for only about 2%. In addition to the RD-AIC channel, neutron stars originating from core-collapse supernovae may also form MSP + sdB systems via the standard recycling process (Wu et al. 2018). Based on BPS simulations in Wu et al. (2020), I estimate that the fraction of eccentric MSP + sdB systems could be as high as 55% among all MSP + sdB binaries, which is significantly larger than the 2% observed for MSP + He WD systems. However, the predicted Galactic population of eccentric MSP + sdB systems is highly sensitive to the lifetime of strongly magnetised MSPs, with 10^8 yr likely representing a conservative upper limit. For instance, magnetars can have characteristic ages as short as 10^3 yr (Igoshev, Popov, & Hollerbach 2021), implying that the expected number of eccentric MSP + sdB systems arising from the RD-AIC scenario may be less than one. Furthermore, the spin-down timescale preceding AIC also plays a critical role in determining the abundance of such systems. In this work, I adopt a pseudo-spin-down timescale of $\tau_{\rm sp} = 10^7$ yr, motivated by observational constraints from type Ia supernovae. In principle, however, $\tau_{\rm sp}$ prior to an AIC event could be considerably longer than 10^7 yr, given the fundamental physical differences between AIC and type Ia explosions. Should $\tau_{\rm sp}$ substantially exceed 10^8 yr, the sdB companion would evolve into a CO WD before AIC occurs. In that case, the RD-AIC channel would not produce eccentric MSP + sdB systems, but rather eccentric MSP/NS + CO WD binaries. Consequently, the numbers predicted here for eccentric MSP + sdB systems should be regarded as a very conservative upper limit. Even if all post-AIC MSPs formed via RD-AIC exhibited lifetimes typical of normal MSPs, the population of eccentric MSP + sdB systems would still be roughly an order of magnitude smaller than that of normal MSP binaries (Bhattacharyya & Roy 2021). Finally, future detections of eccentric MSP + sdB systems may help clarify whether the observed prevalence of very low magnetic fields among MSPs is intrinsic or a selection effect resulting from their longer lifetimes (Freire 2013).

A comparison between the predicted upper limit on the total number of eccentric MSP + sdB binaries in the Galaxy and the currently observed population of such systems could impose a strong constraint on either the lifetime of post-AIC MSPs or the spin-down timescale prior to AIC. Currently, there are approximately 550 known regular MSPs[b] and an underlying population of MSPs of about 83 000 (Levin et al. 2013; Lorimer 2013). Assuming no significant selection effects against their detection, these represent 550/83 000 $\sim$ 0.66% of all regular MSPs in the Galaxy. Based on this detection fraction, and considering that the predicted

[b]https://pages.astro.umd.edu/eferrara/GalacticMSPs.html.

https://doi.org/10.1017/pasa.2026.10189 Published online by Cambridge University Press

orbital characteristics of eccentric MSP + sdB systems are not too extreme, one would expect to observe between 45 and 100 such systems. Yet, none have been detected. This non-detection implies that the lifetime of eccentric MSP + sdB systems formed via AIC could be shorter than 10^6 yr, or alternatively, that the pseudo-spin-down timescale for AIC is close to 10^8 yr. Consequently, based on the observational constraints, the upper limit of the number of such systems could be 1 500.

In such systems, the sdB stars possess masses between 0.38 and 0.65 $M_\odot$, and therefore typically do not undergo a red-giant phase (Justham et al. 2011). Given their relatively long orbital periods, these eccentric MSP + sdB binaries will avoid a stable Roche lobe overflow mass-transfer phase, meaning their orbital eccentricity remains unchanged until they evolve into eccentric NS + CO WD systems. Consequently, the population of eccentric NS + CO WD systems originating from eccentric MSP + sdB progenitors is inherently older than that of the MSP + sdB systems themselves. A future statistical comparison between the observed populations of eccentric MSP + sdB systems and their descendant eccentric NS + CO WD systems could thus provide a meaningful test of the RD-AIC scenario. Regrettably, no systems matching these predictions have yet been identified in the Galactic field.

One question remains to be addressed: why have eccentric MSP + He WD systems been observed, but not eccentric MSP + CO WD systems in Galactic field? Three facts may contribute to this. First, the optimistic estimated number of eccentric MSP + sdB systems, and hence the optimistic number of potential eccentric MSP + CO WD systems originating from the RD–AIC scenario, is at least one order of magnitude smaller than that of eccentric MSP + He WD systems (Wang & Gong 2023). Second, even under the most optimistic estimates for the population of eccentric MSP + sdB systems, the resulting eccentric MSP + CO WD descendants are expected to be rare, since, as discussed earlier, such MSPs are likely to evolve into normal pulsars or neutron stars in graveyards. Additionally, it is crucial to note that the very conservative upper limit of 55% for the eccentric fraction among MSP + sdB systems cannot be directly extrapolated to the MSP + CO WD population. This is because the latter forms through multiple channels, and the RD–AIC scenario likely constitutes only a minor fraction of these systems. (Tauris et al. 2012; Chen & Liu 2013; Wang, Podsiadlowski, & Han 2017; Wang & Liu 2020).

It is widely believed that the MSPs observed in globular clusters (GCs) originate from the AIC channel (van den Heuvel 2010). However, given the advanced ages of GCs, no eccentric MSP + sdB systems have been detected within them to date. Such systems would eventually evolve into a normal pulsar + CO WD stage while retaining their orbital eccentricity. Notably, systems like J1750-3703A and J1824-2452D may represent this population, as they exhibit moderately eccentric orbits, host a slowly rotating pulsar, and have companion mases and orbital periods consistent with theoretical predictions.[c]

Moreover, Podsiadlowski et al. (2005) proposed that if a NS originates from an electron – capture collapse, measuring its mass could help constrain the EoS of NSs by examining the relationship between the pre – collapse and post – collapse masses. Similarly, a pre – AIC to post – AIC mass relation could also constrain the NS EoS, since the AIC process is itself a form of electron - capture collapse. The eccentric MSP + sdB systems, if they are indeed from the RD-AIC scenario, offer a promising avenue for such constraints, as both the pre-AIC and post-AIC masses of the NS may be determined with high precision.

Spinning NSs with non-axisymmetric distortions resulting from solid deformation or excited fluid oscillation modes can emit continuous gravitational waves (CGWs) (Alford & Schwenzer 2015; Chen 2021). An asymmetric rapid RD-AIC event could produce such distortions, potentially leading to detectable CGW signals in future observing runs of Advanced LIGO and Virgo (Abbott et al. 2020). Combined with precise NS mass measurements, the detection of CGWs could offer direct insights into the EoS of NSs (Glampedakis & Gualtieri 2018).

Finally, the results presented here rely on the standard common-envelope wind model, in which several parameters remain highly uncertain, for instance, the adopted CE density (Meng & Podsiadlowski 2017). Given the uncertainties associated with the CE density, the lower limit of the orbital period shown in Figure 2 could be overestimated by up to an order of magnitude.

[c]Please see P. Freire's Web site https://www.naic.edu/pfreire/GCpsr.html.

Acknowledgements. This work is supported by the National Natural Science Foundation of China (Nos. 12288102, 12333008), the Strategic Priority Research Program of the Chinese Academy of Sciences (Grant Nos. XDB1160303, XDB1160000), and the National Science Foundation of China and National Key R&D Program of China (No. 2021YFA1600403). X.M. acknowledges support from Yunnan Fundamental Research Projects (Nos. 202401BC070007 and 202201BC070003), International Centre of Supernovae, Yunnan Key Laboratory (No. 202302AN360001), Yunnan Revitalization Talent Support Program – Yunling Scholar Project and the Yunnan Revitalization Talent Support Program – Science & Technology Champion Project (No. 202305AB350003), and the China Manned Space Program with grant No. CMS-CSST-2025-A13.

Data availability statement. No new data were generated in support of this research, and all the data used in this article will be shared on request to the corresponding author.

References

Abbott, R., et al., 2020, ApJL, 902, L21
Alford, M. G., & Schwenzer, K. 2015, MNRAS, 446, 3631
Alpar, M. A., Cheng, A. F., Ruderman, M. A., & Shaham, J. 1982, Natur, 300, 728
Antoniadis, J. 2014, ApJL, 797, L24
Archibald, A. M., et al. 2009, Sci, 324, 1411
Barr, E. D., et al. 2017, MNRAS, 465, 1711
Bhattacharyya, B., & Roy, J. 2021, Millisecond Pulsars, Astrophysics and Space Science Library (ASSL), ed. S. Bhattacharyya, A. Papitto, & D. Bhattacharya, arXiv: 2104.02294
Bhattacharyya, D., & van den Heuvel, E. P. J. 1991, PhR, 203, 1
Champion, D. J., et al., 2008, Sci, 320, 1309
Chen, L., Meng, X. C., & Han, Z. W. 2017, RAA, 17, 8, 83
Chen, W. C., & Liu, W.M., 2013, MNRAS, 432, L75
Chen, W. C. 2021, PhRvD, 103, 103004
Chen, X. F., Maxted, P. F. L., Li, J., & Han, Z. W. 2017, MNRAS, 467, 1874
Cromartie, H. T., et al. 2020, NatAs, 4, 72
Demorest, P. B., et al., 2010, Natur, 467, 1081
Di Stefano, R., & Kilic, M. 2012, ApJ, 759, 56
Freire, P. C. C., et al. 2011, MNRAS, 412, 2763
Freire, P. C. C. 2013, IAUS, 291, 243
Freire, P. C. C., & Tauris, T. M. 2014, MNRAS, 438, L86
Glampedakis, K., & Gualtieri, L. 2018, in The Physics and Astrophysics of Neutron Stars, Astrophysics and Space Science Library, Vol. 457, ed. L. Rezzolla et al. (Dordrecht: Springer), 673

Geier, S., et al. 2011, in AIP Conference Proceedings, ed. S. Schuh, H. Drechsel, & U. Heber, 1331, 163
Geier, S. et al. 2015, Sci, 347, 1126
Geier, S., et al. 2017, A&A, 600, A50
Ginzburg, S., & Chiang, E. 2022, MNRAS, 509, L1
Götberg, Y., et al. 2020, ApJ, 904, 14
Guo, Y., Wang, B., & Li, X. 2024, MNRAS, 527, 7394
Guo, Y., Wang, B., Li, X., Liu, D., & Tang, W. 2025, arXiv: 2505.16299
Hachisu, I., Kato, M., Saio, H., & Nomoto, K. 2012, ApJ, 744, 69
Han, Q. & Li, X. D. 2021, ApJ, 909, 161
Han, Z., Podsiadlowski, P., & Lynas-Gray, A. E. 2007, MNRAS, 380, 1098
Han, Z., Podsiadlowski, PH., Maxted, P. F. L., & Marsh, T. R. 2003, MNRAS, 341, 669
He, R., Meng, X., Lei, Z., Yan, H., & Lan, S. 2025, A&A, 693, A121
Heber, U., 2009, ARA&A, 47, 211
Heber, U. 2016, PASP, 128, 082001
Hills, J. G. 1983, ApJ, 267, 322
Hurley, J. R., Pols, O. R., & Tout, C. A. 2000, MNRAS, 315, 543
Hurley, J. R., Tout, C. A., & Pols, O. R. 2002, MNRAS, 329, 897
Ivanova, N., Heinke, C. O., Rasio, F. A., Belczynski, K., & Fregeau, J. M. 2008, MNRAS, 386, 553
Igoshev, A. P., Popov, S. B., & Hollerbach, R. 2021, Universe, 7, 351
Jiang, L., et al. 2015, ApJ, 807, 41
Justham, S. 2011, ApJL, 730, L34
Justham, S., Podsiadlowski, PH., & Han, Z. 2011, MNRAS, 410, 984
Kremer, K., et al. 2024, ApJ, 977, L42
Lattimer, J. M., & Yahil, A. 1989, ApJ, 340, 426
Levin, L., et al. 2013, MNRAS, 434, 1387
Lorimer, D. R. 2013, IAUS, 291, 237
Manchester, R. N., et al. 2005, AJ, 129, 1993
Meng, X., & Li, J. 2019, MNRAS, 482, 5651
Meng, X., & Luo, Y. 2021, MNRAS, 507, 4603
Meng, X., & Podsiadlowski, PH. 2013, ApJL, 778, L35
Meng, X., & Podsiadlowski, PH. 2017, MNRAS, 469, 4763
Meng, X., & Podsiadlowski, PH. 2018, ApJ, 861, 127
Moehler, S., Richtler, T., de Boer, K. S., Dettmar, R. J., & Heber, U. 1990, A&AS, 86, 53
Octau, F., et al. 2018, A&A, 612, A87
Özel, F. & Freire, P. 2016, ARA&A, 54, 401
Oostrum, L. C., van Leeuwen, J., Maan, Y., Coenen, T., & Ishwara-Chandra, C. H. 2020, MNRAS, 492, 4825
Phinney, E. S., & Kulkarni, S. R. 1994, ARA&A, 32, 591
Podsiadlowski, PH., Dewi, J. D. M., Lesaffre, P., Miller, J. C., Newton, W. G., & Stone, J. R. 2005, MNRAS, 361, 1243
Prada Moroni, P. G., & Straniero, O. 2009, A&A, 507, 1575
Radhakrishnan, V., & Srinivasan, G. 1982, CSci, 51, 1096
Serylak, M., et al. 2022, A&A, 665, A53
Stovall, K., et al. 2019, ApJ, 870, 74
Tang, W.-S., Gao, S.-J., & Li, X.-D. 2023, MNRAS, 519, 2951
Tauris, T. M., Langer, N., & Kramer, M. 2012, MNRAS, 425, 1601
Tauris, T. M., Sanyal, D., Yoon, S. C., & Langer, N. 2013, A&A, 558, A39
van den Heuvel, E. P. J. 2010, NewAR, 54, 140
Wang, B. 2018, MNRAS, 481, 439
Wang, B., & Liu, D. D. 2020, RA&A, 20,135
Wang, B., Podsiadlowski, PH., & Han, Z. 2017, MNRAS, 472, 1593
Wang, D., & Gong, B. P. 2023, MNRAS, 526, 5021
Wickramasinghe, D. T., & Ferrario, L. 2005, MNRAS, 356, 1576
Wijnands, R., & van der Klis, M. 1998, Natur, 394, 344
Wu, Y., Chen, X., Li, Z., & Han, Z. 2018, A&A, 618, A14
Wu, Y., Chen, X., Chen, H., Li, Z., & Han, Z. 2020, A&A, 634, A126
Yang, Z. L., et al. 2025, Sci, 388, 859
Yoon, S.-C., & Langer, N. 2004, A&A, 419, 623
Yoon, S.-C., & Langer, N. 2005, A&A, 435, 967
Zhu, W. W., et al. 2019, ApJ, 881, 165

https://doi.org/10.1017/pasa.2026.10189 Published online by Cambridge University Press